Supporting Information

Karashima *et al*. 10.1073/pnas.0808487106

SI Methods

Patch-Clamp Recordings. Recordings were made by using EPC-7 or EPC-9 patch-clamp amplifiers (HEKA Elektronik) and patchmaster (HEKA Elektronik) or pClamp 9 (Molecular Devices) software. Data were sampled at 5–20 kHz and filtered offline at 1–5 kHz. Between 50% and 80% of the series resistance was compensated. The standard extracellular recording solution contained (in mM) 150 NaCl, 1 $MgCl_2$, 1.5 $CaCl_2$ 10 glucose, and 10 Hepes (pH 7.4 with NaOH). In the Ca^{2+}-free extracellular solution, $CaCl_2$ was omitted and 1 mM EGTA was added. The intracellular standard pipette solution contained (in mM) 150 CsCl, 1 $MgCl_2$, 10 1,2-bis(*o*-aminophenoxy)ethane-*N*,*N*,*N*′,*N*′-tetraacetic acid (BAPTA), and 10 Hepes (pH 7.2 with CsOH). To obtain a pipette solution with 10 μM free Ca^{2+} and 1 mM free Mg^{2+}, the high-affinity Ca^{2+} chelator BAPTA was replaced by 10 mM lower-affinity chelator *N*-(2-hydroxyethyl)ethylenedinitrilotriacetic acid (HEDTA), and the appropriate amounts of $CaCl_2$ and $MgCl_2$ were added (1.36 mM and 9.1 mM, respectively). In cell-attached recordings, NaCl in the extracellular solution was replaced with KCl, and the standard extracellular recording solution was used as pipette solution.

MO, menthol, capsaicin, CLT, thapsigargin, and CPA were purchased from Sigma–Aldrich. MO, CLT, thapsigargin, and CPA were dissolved in DMSO, and menthol and capsaicin in ethanol.

Behavioral Assays. Weight-matched, 10- to 13-week-old mice were used in the behavioral experiments. WT and *Trpa1*$^{-/-}$ mice were housed under identical conditions, with a maximum of 4 animals per cage on a 12 h light–dark cycle and with food and water ad libitum. For the cold plate test, a Hot Cold Plate Analgesia Meter (IITC Co.) was used. Mice were placed on a plate with surface temperature maintained at 30°C, 10°C, or 0°C, and the behavior was recorded by using a digital video camera. Nocifensive behavior was quantitatively evaluated (without knowledge of the genotype) by counting the number of jumps during a 2-min period and by analysis of the latency to the first jump and to the first cold-induced behavioral response. For the tail-flick experiments, mice were firmly held above a water–methanol mixture at −10°C with the distal half of the tail submerged in the fluid. The time until tail withdrawal was measured with a cutoff time of 60 s. The mice were accustomed to this course of action by performing a similar procedure but with the fluid set at 37°C in the 2 days preceding the −10°C stimulus. Mice did not exhibit any tail flicking in this condition within the cutoff time (60 s).

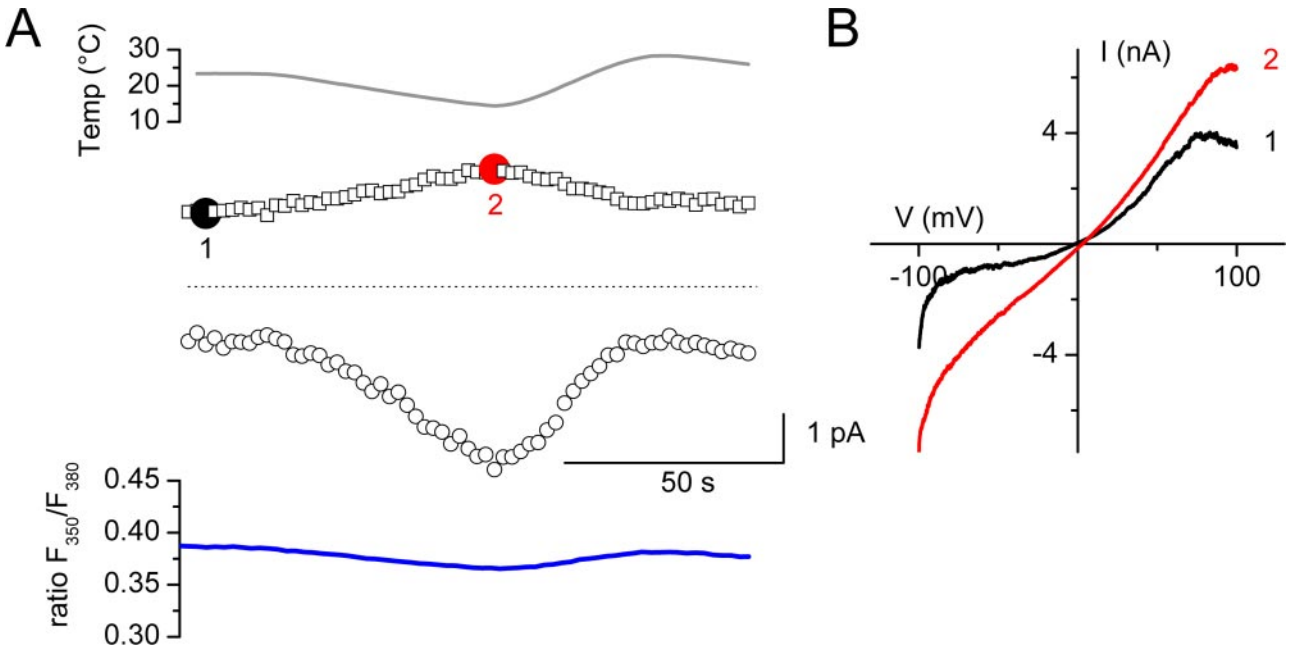

Fig. S1. Simultaneous recording of intracellular Ca^{2+} changes and cold-activated, whole-cell TRPA1 currents in CHO cells. (*A*) Time course of whole-cell TRPA1 currents at +50 and −75 mV and of the ratio of Fura-2 fluorescence upon illumination at 350 and 380 nm, during cooling. Recording conditions were identical to those in Fig. 1*B*, except for the addition of 100 μM Fura-2 K^+ salt to the Ca^{2+}-free pipette solution. The starting point of the recording was 180 s after establishment of the whole-cell configuration. From the time course of the fluorescence signal at an excitation wavelength of 380 nm, we obtained a monoexponential time constant for the loading of Fura-2 of 90 ± 15 s ($n = 4$). Given the structural relation between Fura-2 and BAPTA, this time constant can be considered an upper limit of the time course of BAPTA loading into the cells. (*B*) Current–voltage relations obtained at the indicated time points. This recording is representative for 4 similar experiments.

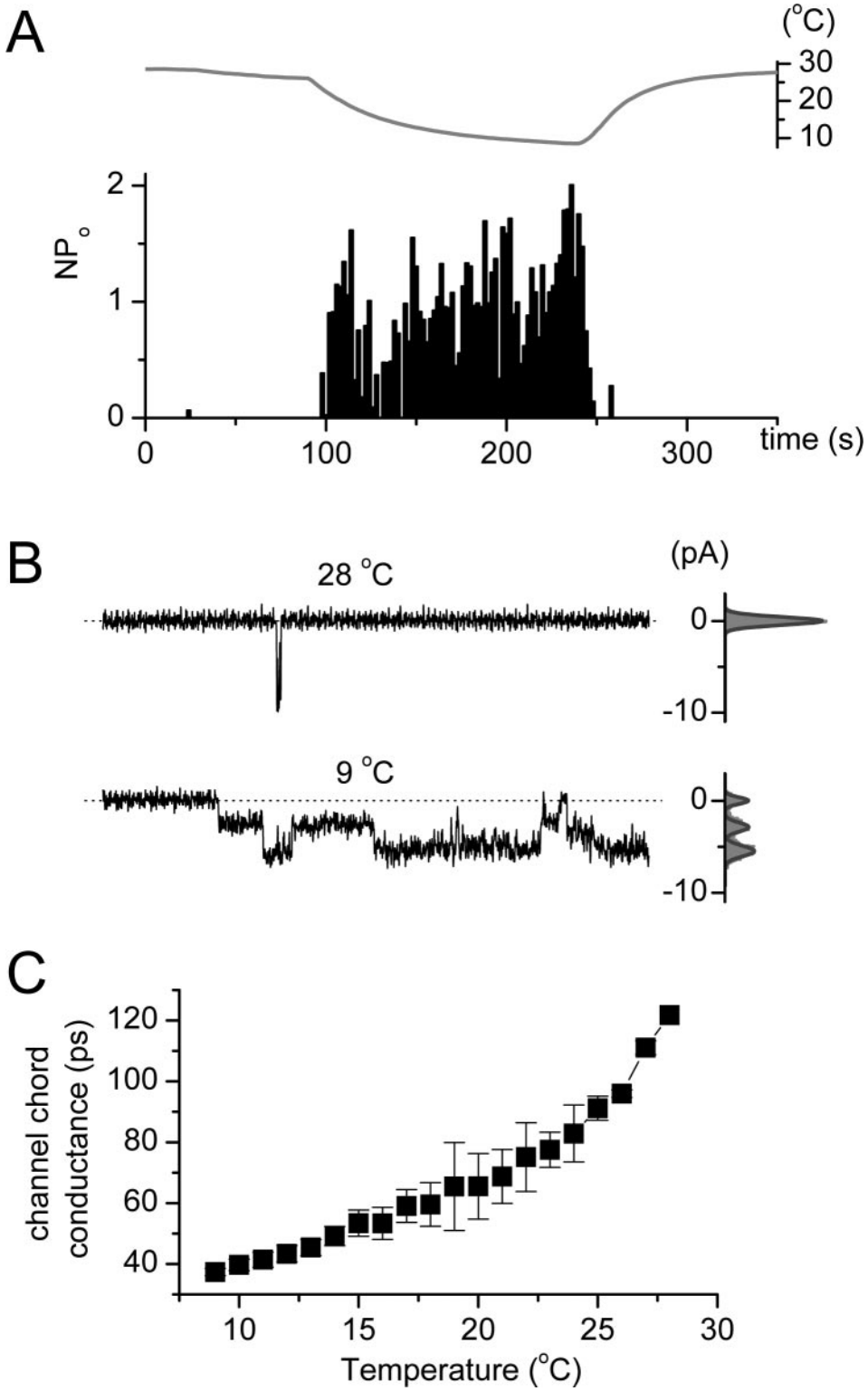

Fig. S2. Cold-activated TRPA1 single-channel currents in cell-attached patches. (*A*) Time course of NP_{open} at −100 mV during transient cooling. (*B*) Representative 1-s current recordings at 28°C and 9°C. (*C*) Temperature dependence of the TRPA1 single-channel conductance ($n = 5$).

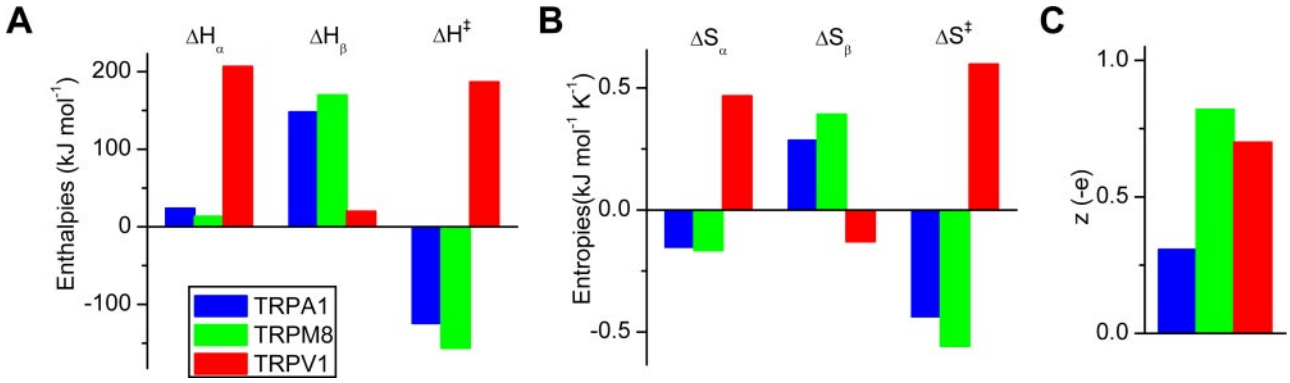

Fig. S3. Thermodynamics of TRPA1 gating. Comparison of the changes in enthalpy and entropy, as well as the equivalent gating charge used to describe gating of TRPA1, TRPM8, and TRPV1. To quantitatively describe the temperature dependence of TRPA1 gating, we used a 2-state gating model:

$$Closed \underset{\beta(V,T)}{\overset{\alpha(V,T)}{\rightleftharpoons}} Open.$$

The forward and backward rates are determined by Eyring rate theory:

$$\alpha(V, T) = \frac{kT}{h} \exp\left(-\frac{\Delta H_\alpha}{RT} + \frac{\Delta S_\alpha}{R} + \frac{zF\delta V}{RT} \right),$$

$$\beta(V, T) = \frac{kT}{h} \exp\left(-\frac{\Delta H_\beta}{RT} + \frac{\Delta S_\beta}{R} - \frac{zF(1-\delta)V}{RT} \right)$$

where k is the Boltzmann constant (1.38×10^{-23} J·K^{-1}), h the Planck constant (6.63×10^{-34} J), ΔH_i and ΔS_i ($i = \alpha,\beta$) the enthalpy and entropy (per mole) charges associated with each transition, z the effective charge associated with voltage-dependent gating, and δ the electrical coupling factor (which was set to 0.5). Estimates for the changes in enthalpy and entropy (ΔH_i and ΔS_i) were obtained by a global fit of the model to the experimental relaxation time constants and tail currents at different voltages and temperatures.

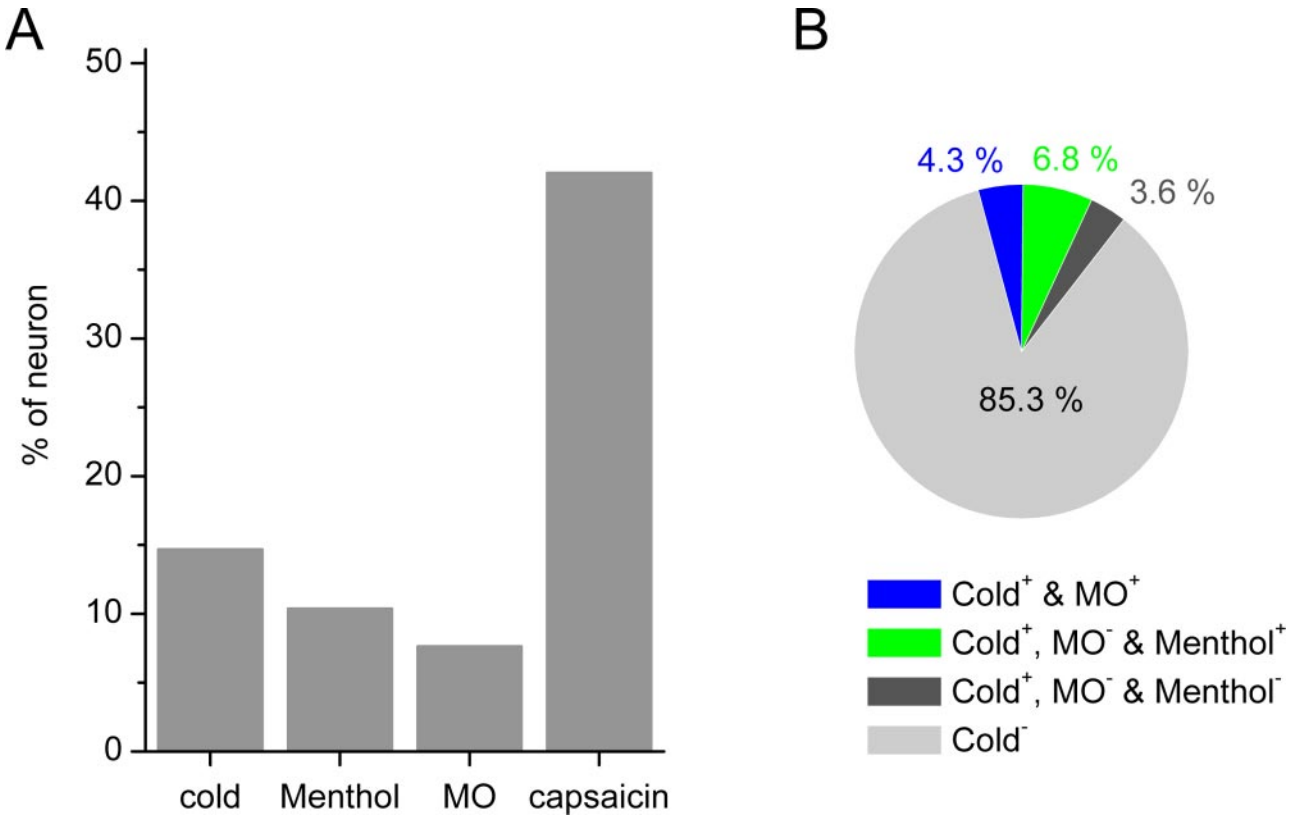

Fig. S4. Reduced TRPA1-mediated cold responses in TG neurons from newborn WT mice ($n = 695$ from 13 mice). (*A*) Percentage of cells responding to cold and chemical stimuli in preparations from newborn WT mice. (*B*) Pie charts showing the percentage of cold-insensitive and the 3 types of cold-sensitive neurons in TG from newborn WT mice.

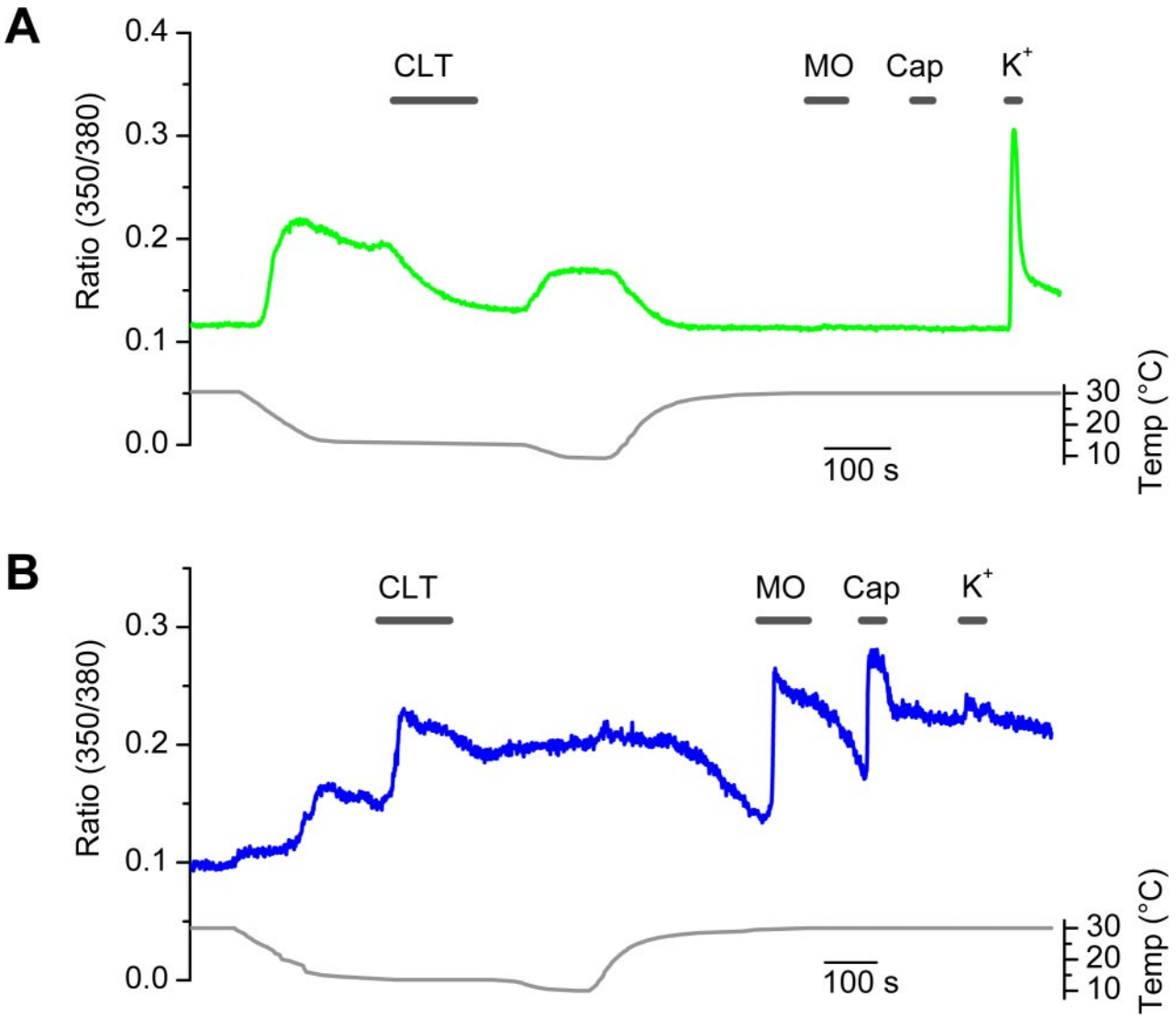

Fig. S5. Effects of clotrimazole (CLT) on cold-sensitive TG neurons from adult WT mice. (*A*) Inhibitory effect of CLT (10 μM) on the cold response in an MO-insensitive, menthol-sensitive TG neuron. (*B*) Stimulatory effect of CLT (10 μM) on the cold response in an MO-sensitive TG neuron.

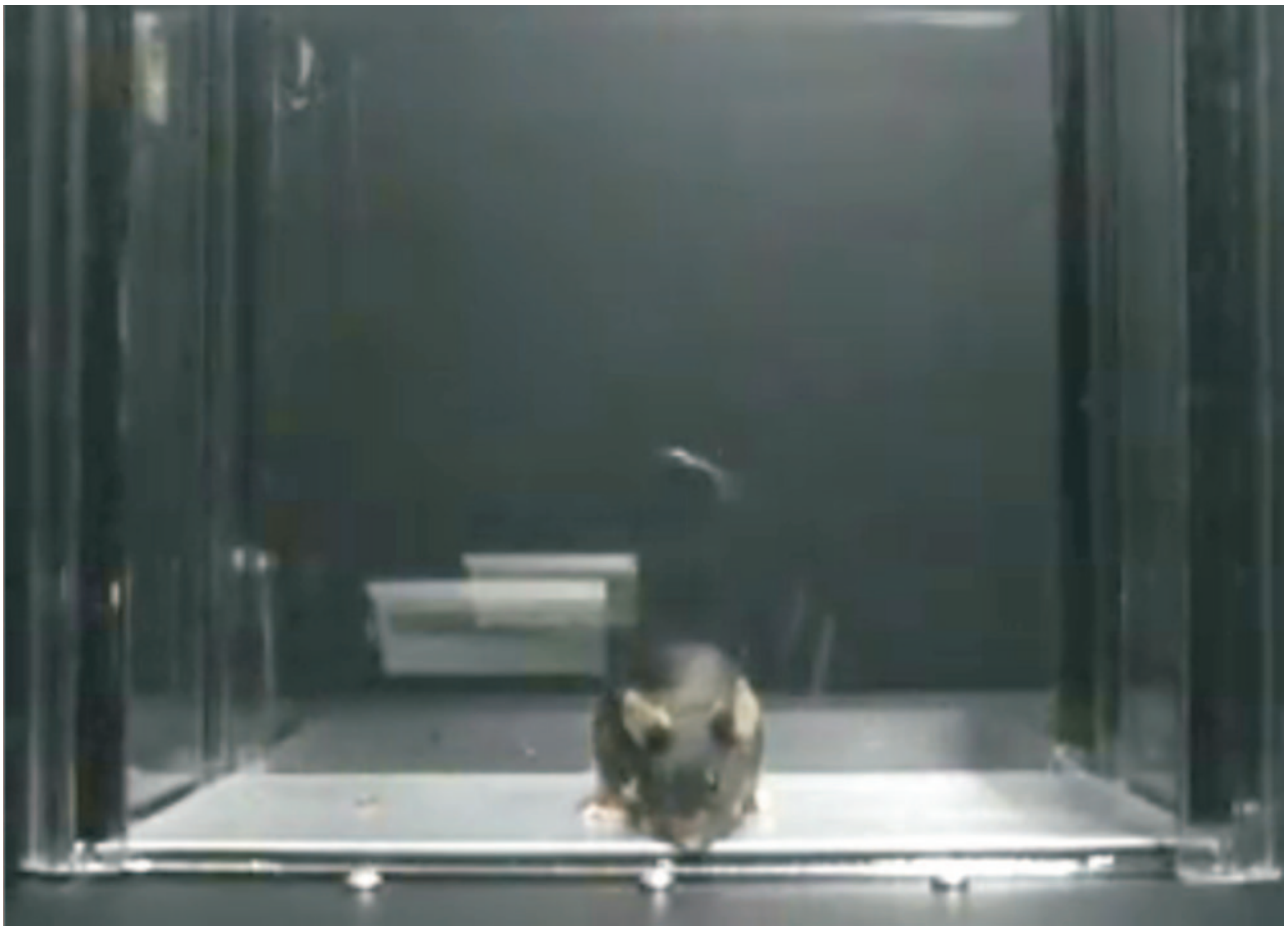

Movie S1. Illustration of the typical behavior of WT and *Trpa1*$^{-/-}$ mice when placed on a cold plate set at 30°C and 0°C.

Movie S1 (MP4)